Crystal-field interaction in the pyrochlore magnet Ho₂Ti₂O₇

S. Rosenkranz[a)]
Materials Science Division, Argonne National Laboratory, Argonne, Ilinois 60439

A. P. Ramirez
Bell Laboratories, Lucent Technologies, 600 Mountain Avenue, Murray Hill, New Jersey 07974

A. Hayashi and R. J. Cava
Chemistry Department, Princeton University, Princeton, New Jersey 08540

R. Siddharthan and B. S. Shastry
Department of Physics, Indian Institute of Science, Bangalore 560012, India

Neutron time-of-flight spectroscopy has been employed to study the crystal-field interaction in the pyrochlore titanate $Ho_2Ti_2O_7$. The crystal-field parameters and corresponding energy-level scheme have been determined from a profile fit to the observed neutron spectra. The ground state is a well separated E_g doublet with a strong Ising-like anisotropy, which can give rise to frustration in the pyrochlore lattice. Using the crystal-field parameters determined for the Ho compound as an estimate of the crystal-field potential in other pyrochlore magnets, we also find the Ising type behavior for Dy. In contrast, the almost planar anisotropy found for Er and Yb prevents frustration, because of the continuous range of possible spin orientations in this case. © *2000 American Institute of Physics.* [S0021-8979(00)22908-3]

I. INTRODUCTION

Pyrochlore rare-earth titanates $R_2Ti_2O_7$ (R=rare earth) have attracted much interest recently because their structure of corner-sharing tetrahedra can lead to geometrical frustration, i.e., the suppression of long-range magnetic order arising from the incompatibility of local and global symmetries.[1] In the case of isotropic Heisenberg exchange interactions, the Pyrochlore lattice can exhibit frustration for the antiferromagnet.[2,3] However, frustration occurs even for ferromagnetic interactions when the spins lie along an axis joining the tetrahedron vertex with its center (Ising limit).[4–6] Depending on the relative importance of the exchange interaction, single-ion anisotropy, and classical dipolar interaction, the pyrochlore titanates exhibit various interesting low temperature properties including cooperative paramagnetism, long-range order, partial order with a sharp transition to paramagnetism, and high disorder with a broad transition to paramagnetism.[4–11] The latter has been termed ''spin ice,'' in analogy to the large ground-state degeneracy arising from local rules for the ordering of protons in common water ice (ice I_h).[4]

In the pyrochlore titanates, a strong single-ion anisotropy imposed by the crystal field (CF) interaction may force the rare-earth spins into the Ising limit. However, despite it's importance in determining the possibility of frustration, the CF interaction in the pyrochlores has to date not been investigated by direct spectroscopic methods. We therefore carried out inelastic neutron time-of-flight experiments on $Ho_2Ti_2O_7$ and determined the CF parameters from profile fits to the observed spectra. The ground state is an almost pure $|J,J_z\rangle \approx |8, \pm 8\rangle$ doublet, well separated from the first excited state at 20.4 meV, with a strong easy-axis anisotropy $\chi_z / \chi_\perp$

$\sim$350 at $T=10$ K. Although this Ising-like behavior can give rise to frustration,[4] it has recently been shown that the inclusion of the dipolar and superexchange interaction results in a partially ordered state at low temperature, and not in a highly disordered spin ice.[11]

II. EXPERIMENTAL RESULTS

The $Ho_2Ti_2O_7$ sample was prepared as a ceramic powder following standard solid-state synthesis techniques as described in Ref. 9. Approximately 5 g of the sample was enclosed in a thin-walled aluminum container with a flat-plate geometry of 7×2.5 cm^2 and mounted into a closed-cycle refrigerator on the neutron time-of-flight spectrometer LRMECS at the spallation source IPNS at Argonne National Laboratory. In order to minimize self-shielding at higher angles, the sample was mounted at a 45° angle with respect to the incident beam. Spectra were recorded at incident energies $E_i = 120$, 35, and 6 meV and at temperatures $T=10$, 75, and 150 K, respectively. The raw data were normalized and corrected for detector efficiency and time-independent background following standard procedures. The instrumental resolution was determined for each incident energy using monochromatic vanadium runs. These vanadium runs were also used to normalize the scattering intensity observed at different incident energies, leaving only one overall scale factor in the data analysis.

The free ion ground-state J multiplet $^5I_8$ of the Ho^{3+} ion in $Ho_2Ti_2O_7$ splits in the crystal field of D_{3d} symmetry into ten states:[12] five E_g doublets, three A_{1g}, and two A_{2g} singlets, as indicated in Fig. 1. Choosing the quantization axis along the $\langle 111 \rangle$ direction of the crystallographic cell, the CF Hamiltonian takes the form
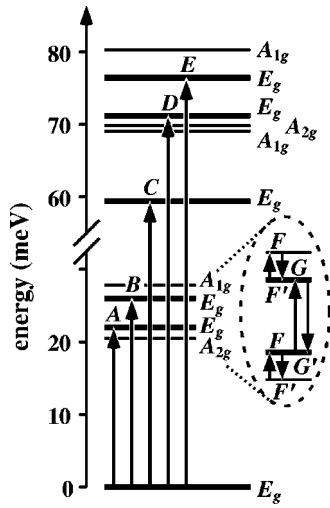
[a)]Electronic mail: srosenkranz@anl.gov

FIG. 1. CF energy level scheme for the Ho^{3+} ion in Ho$_2$Ti$_2$O$_7$. The arrows denote observed transitions.

$$\mathcal{H}_{CF} = B_0^2 C_0^2 + B_0^4 C_0^4 + B_3^4(C_3^4 - C_{-3}^4)$$
$$+ B_0^6 C_0^6 + B_3^6(C_3^6 - C_{-3}^6) + B_6^6(C_6^6 + C_{-6}^6), \tag{1}$$

where B_q^k denote the CF parameters and C_q^k are the components of the tensor operator C^k as defined in Ref. 13. Here, we treat the CF interaction in the LS coupling scheme as a perturbation within the ground-state J multiplet only.

The unpolarized neutron scattering cross-section for a transition from the CF state $|i\rangle$ to $|j\rangle$ is in the dipole approximation given by[14]

$$\frac{\partial^2 \sigma}{\partial \Omega \partial \omega} = N\left(\frac{\gamma e^2}{m_e c^2}\right)^2 \frac{k_1}{k_0} f^2(Q) e^{-2W} \rho_i$$
$$\times |\langle j|\mathbf{m}_p|i\rangle|^2 \delta(E_i - E_j + \hbar\omega), \tag{2}$$

where $\hbar\omega$ denotes the energy transferred from the neutron to the sample, e^{-2W} the Debye–Waller factor, $f(Q)$ the magnetic formfactor, ρ_i the occupancy of the state $|i\rangle$ with energy E_i, and $\mathbf{m}_p$ the component of the magnetic-moment operator perpendicular to the scattering vector $\mathbf{Q}$. The remaining symbols have their usual meaning. The distinct dependence of the scattering intensity of CF transitions on temperature and momentum transfer, c.f. Eq. (2), allows to distinguish them from other excitations, like phonons.

Figure 2 shows energy spectra observed for Ho$_2$Ti$_2$O$_7$. At 10 K, there are clearly visible transitions A-E, which all decrease in intensity with increasing momentum transfer (as shown in Fig. 3 for the transition C) and increasing temperature (see Fig. 2) and are therefore identified as ground-state CF transitions. At higher temperatures, additional transitions F, F', G, and G' from excited states are observed. An unambiguous assignment of these observed transitions to a level scheme is however not possible because the powder average of the cross section Eq. (2) does not yield unique selection rules in the given symmetry. We have therefore employed the following procedure in order to obtain a reliable quantization of the CF interaction. First, the CF parameters B_q^k were parametrized as[15]
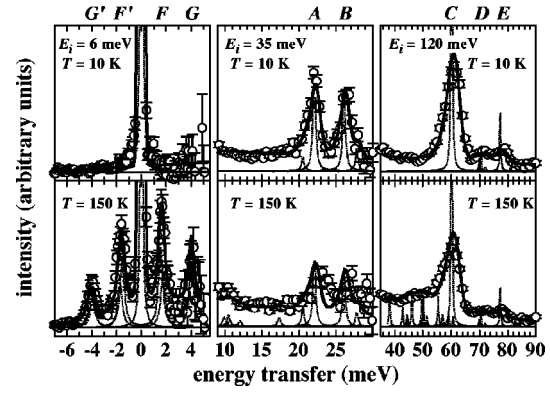

FIG. 2. Energy spectra for Ho$_2$Ti$_2$O$_7$ measured on LRMECS. The solid line denotes the calculated spectra using the best fitted CF parameters, including an intrinsic Lorentzian broadening of the transitions as well as the instrumental resolution. The dotted lines denote the individual, Lorentzian broadened CF transitions.

$$B_q^k = WF_{kq}x_{kq}, \tag{3}$$

where $F_{20} = 3600$, $F_{40} = 4004$, $F_{43} = 527\sqrt{35}$, $F_{60} = 1784.64$, $F_{63} = 118.976\sqrt{105}$, and $F_{66} = 81.12\sqrt{231}$,[16] and W is an overall scale factor determining the total splitting of the ground-state J multiplet. This parametrization is advantageous because the range of the parameters x_{kq} is limited by the condition

$$\sum_{k,q} |x_{kq}| = 1, \tag{4}$$

thus allowing a scan of the entire parameter space $\{x_{kq}\}$ for sets that describe well the observed spectra. After a comprehensive stepwise search, we found that only a restricted region of the parameter space is consistent with the observed data. In a second step, we used a least-squares procedure to refine the CF parameters in profile fits to the observed energy spectra shown in Fig. 2, taking into account the instrumental resolution function and allowing for an intrinsic Lorentzian broadening of the individual CF transitions. Using different sets within the region found in the first step as start parameters, we always arrived at the same resulting CF parameters (in meV) $B_0^2 = 68.2 \pm 1.1$, $B_0^4 = 274.8 \pm 1.7$, $B_3^4 = 83.7 \pm 1.1$, $B_0^6 = 86.8 \pm 0.8$, $B_3^6 = -62.5 \pm 0.6$, and $B_6^6 = 101.6 \pm 1.2$,[17] which give an overall good agreement with the observed
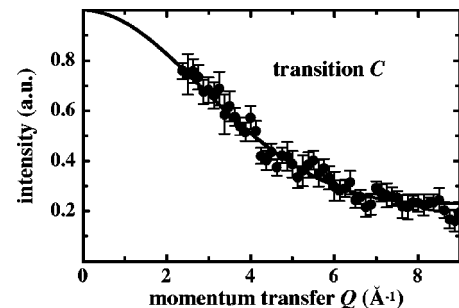

FIG. 3. Q dependence of the scattering intensity integrated over the energy transfer $\hbar\omega = 60 \pm 1$ meV (transition C). The solid line denotes the square of the magnetic formfactor, $f^2(Q)$, for Ho^{3+} in the dipole approximation on top of a flat background.

spectra, as seen in Fig. 2. The reliability of these parameters can be verified by comparing our results with other pyrochlores: Since the crystal structure varies only little on replacing one rare earth with another, the CF parameters determined for R=Ho should also give a good estimate of the CF interaction in the other compounds.[18] In particular, we obtain for Tb a ground-state E_g doublet followed by an E_g doublet at 1.5 meV and two singlets A_{2g} at 12 meV and A_{1g} at 18 meV, respectively, and for Tm a ground-state A_{2g} singlet followed by an E_g doublet at 11.5 meV, in good agreement with neutron-scattering experiments.[8,19]

III. DISCUSSION

The strong CF interaction in the pyrochlore titanates, with overall splittings of the ground-state J multiplets in the order of 100 meV, is important in determining the collective low-temperature behavior, since it may impose restrictions on the possible orientations of the rare-earth spins. The occurrence of such restrictions can be easily inspected from the single-ion susceptibility

$$\chi^{\alpha\alpha} = \sum_{\substack{i,j \\ E_j = E_i}} \frac{|\langle i|m^\alpha|j\rangle|^2}{k_B T} \rho_i$$
$$+ \sum_{\substack{i,j \\ E_j \neq E_i}} \frac{|\langle i|m^\alpha|j\rangle|^2}{E_j - E_i}(\rho_i - \rho_j), \tag{5}$$

where m^α denotes the α component of the magnetic moment operator and $|i\rangle$ and E_i are the eigenfunctions and energies of the CF Hamiltonian Eq. (1). For the Ho compound, the ground state is a well separated E_g doublet (see Fig. 1), composed almost entirely of the $|J,J_z\rangle = |8,\pm 8\rangle$ states. Although the admixture of other states in the correct ground-state wave function and the inclusion of excited states in Eq. (5) will lead to a deviation from a pure Ising behavior, the calculated anisotropy $\chi_z/\chi_\perp \sim 350$ at $T=10$ K shows that the Ising limit is a good approximation. Nevertheless, $Ho_2Ti_2O_7$ is not a spin ice, but shows partial order at low temperatures because of dipolar and antiferromagnetic superexchange interactions.[11]

For a discussion of the anisotropy in other rare-earth titanates, we make again use of the CF parameters determined for Ho as an estimate of the CF interaction in the other compounds.[18] For Dy, we find a very similar situation

as observed for Ho, i.e., a strong easy-axis anisotropy $\chi_z/\chi_\perp \sim 300$ at $T=10$ K. For this compound, which has been shown to be a good realization of the spin-ice model,[9] the ground state is an almost pure $|15/2,\pm 15/2\rangle$, (S_1,S_3) Kramers doublet, separated from the first excited state by ≈ 33 meV. In contrast, for R=Er and Yb the CF interaction gives rise to a planar XY-like anisotropy $\chi_z/\chi_\perp \approx 1/5$ at $T=10$ K. In this case, the continuous range of possible spin orientations prevents frustration. Another interesting case is Tb, which shows cooperative paramagnetism at low temperature.[8] Here, the ground-state E_g doublet is only separated by 1.5 meV from the next E_g doublet. As a result, we find a weak easy-axis anisotropy $\chi_z/\chi_\perp \sim 3$ down to $T \approx 10$ K, which only exceeds $\chi_z/\chi_\perp > 10$ below $T \sim 1$ K.

[1] A. P. Ramirez, Annu. Rev. Mater. Sci. **24**, 453 (1994).
[2] B. D. Gaulin *et al.*, Phys. Rev. Lett. **69**, 3244 (1992).
[3] R. Moessner and J. T. Chalker, Phys. Rev. B **58**, 12049 (1998).
[4] M. J. Harris *et al.*, Phys. Rev. Lett. **79**, 2554 (1997).
[5] R. Moessner, Phys. Rev. B **57**, R5587 (1998).
[6] S. T. Bramwell and M. J. Harris, J. Phys.: Condens. Matter **10**, L215 (1998).
[7] M. J. Harris *et al.*, Phys. Rev. Lett. **81**, 4496 (1998).
[8] J. S. Gardner *et al.*, Phys. Rev. Lett. **82**, 1012 (1999).
[9] A. P. Ramirez *et al.*, Nature (London) **399**, 333 (1999).
[10] N. P. Raju *et al.*, Phys. Rev. B **59**, 14489 (1999).
[11] R. Siddharthan *et al.*, Phys. Rev. Lett. **83**, 1854 (1999).
[12] We follow the symmetry notation of J. L. Prather, *Atomic Energy Levels in Crystals*, National Bureau of Standards monograph **19** (Washington, U.S. Dept. of Commerce, National Bureau of Standards, 1961), which is a modification of Mullikens notation used in molecular spectroscopy.
[13] B. G. Wybourne, *Spectroscopic Properties of Rare Earths* (Interscience, New York, 1965).
[14] G. T. Trammell, Phys. Rev. **92**, 1387 (1953).
[15] U. Walter, J. Phys. Chem. Solids **45**, 401 (1984).
[16] The factors given here correspond to the inverse of the factors given in Ref. 15, transformed to the tensor-operator formalism utilized in the present work.
[17] In this choice, the reference frame for the CF Hamiltonian is related to the crystallographic axes through a rotation by the Euler angles $\alpha=0$, $\cos\beta=\sqrt{3}/3$, and $\gamma=45°$.
[18] In the extrapolation of the CF parameters from one rare-earth to another, we included a standard correction for $\langle r^k \rangle$, the kth moment of the radial distribution of the $4f$ electrons.
[19] M. P. Zinkin, M. J. Harris, Z. Tun, R. A. Cowley, and B. M. Wanklyn, J. Phys.: Condens. Matter **8**, 193 (1996).